Multiplexed detection of xylene and trichloroethylene in water by photonic crystal absorption spectroscopy

Wei-Cheng Lai,[1] Swapnajit Chakravarty,[2,*] Yi Zou,[1] and Ray T. Chen[1,3]

[1]*Department of Electrical and Computer Engineering, University of Texas at Austin, Austin, Texas 78712, USA*

[2]*Omega Optics Inc., Austin, Texas 78759, USA*

[3]*e-mail: raychen@uts.cc.utexas.edu*

**Corresponding author: swapnajit.chakravarty@omegaoptics.com*

Received July 18, 2013; revised August 15, 2013; accepted August 27, 2013;
posted August 29, 2013 (Doc. ID 194005); published September 20, 2013

We experimentally demonstrate simultaneous selective detection of xylene and trichloroethylene (TCE) using multiplexed photonic crystal waveguides (PCWs) by near-infrared optical absorption spectroscopy on a chip. Based on the slow light effect of photonic crystal structure, the sensitivity of our device is enhanced to 1 ppb (v/v) for xylene and 10 ppb (v/v) for TCE in water. Multiplexing is enabled by multimode interference power splitters and Y-combiners that integrate multiple PCWs on a silicon chip in a silicon-on-insulator platform.

OCIS codes: (230.5298) Photonic crystals; (130.6010) Sensors; (130.5296) Photonic crystal waveguides.
http://dx.doi.org/10.1364/OL.38.003799

Infrared (IR) absorption spectroscopy is widely accepted as the ideal technique for chemical sensing due to the unique capability to distinguish analytes of interest based on unique molecular vibration signatures [1,2]. In this respect, IR spectroscopy has an overwhelming practical advantage over optical methods that depend on sensing changes in refractive index which are not very different when comparing organic substances for instance, volatile organic compounds (VOCs) in water. Commercially available IR spectroscopy systems based on tunable diode laser absorption spectroscopy (TDLAS) [1] or Fourier transform infrared (FTIR) spectroscopy [2] are benchtop systems primarily for measuring gases and are unsuitable for *in situ*, continuous, remote monitoring in water ambient.

We have previously demonstrated that in photonic crystal (PC) slot waveguide-based on-chip absorption spectroscopy [3,4], the optical absorption path length is significantly enhanced compared to free space, thereby leading to enhanced light–matter interaction. As a result, significantly better sensitivities are achieved compared to optical-fiber-based methods [5,6]. Using the aforementioned method, we successfully detected xylene directly in water down to a concentration of 100 ppb (parts per billion) [3] and also detected methane in air down to a concentration of 100 ppm (parts per million) [4] with a 300 μm long PC slot waveguide. Measurements involved optical-fiber-coupled light input and output from the sensing waveguides. Measurements and device packaging considerations are thus obviously simpler than microgas-chromatography-based sensors [7,8] that are limited to compounds that are sufficiently volatile, thermally stable during heating, and also volatilizes at temperatures that do not exceed thermal handling capabilities of the column packing. Device packaging is complicated by the need to have heating elements integrated with the chip. Furthermore, in gas chromatography (GC), microgas chromatography (μGC), and alternative chip-based optical methods for VOC sensing, refractive index changes [9–11] are maximized in a functional polymer for a certain VOC or groups of VOCs. In on-chip absorption spectroscopy, a hydrophobic polymer with optical transparency in the absorbance wavelength range of interest of the VOC is needed. However, a single hydrophobic polymer such as SU-8 or poly-dimethyl siloxane (PDMS) can be integrated to measure a significant number of VOCs in the near-IR since the VOCs are uniquely identified by their respective unique absorbance signatures in the near-IR.

GC and its corresponding chip-based μGC obviously have the advantage of multiplexed detection. While multiplexing can be achieved by integrating several parallel PC slot waveguides with an optical fiber array at the input and the output, packaging of commercially available optical fiber arrays would increase complexity and cost. In this Letter, we experimentally demonstrate an integrated-optics-based method for simultaneous multiplexed detection of two VOCs, xylene and TCE with PC waveguides (PCWs) using a single optical fiber input and output. We also demonstrate that high sensitivities down to 1 ppb for xylene and 10 ppb for TCE are achieved by using SU-8 as the film for solid-phase microextraction (SPME) instead of PDMS; two orders of magnitude better than our previous demonstration [3] and more than an order of magnitude better than other technologies [7,8,12–14].

The device is fabricated in silicon in a silicon-on-insulator (SOI) substrate using standard e-beam lithography and reactive ion etching [3]. The principle of operation of our device is governed by the Beer–Lambert law for optical absorption spectroscopy. According to this law, the transmitted intensity I is given by

$$I = I_0 \times \exp(-\gamma \alpha L), \tag{1}$$

where I_0 is the incident intensity, γ is the absorption coefficient of the medium, L is the interaction length, and α is the medium-specific absorption factor determined by dispersion-enhanced light–matter interaction. For various applications, L must be large to achieve high sensitivity since $\alpha = 1$.

In addition, from perturbation theory

$$\gamma \propto f \times \frac{c/n}{v_g}, \tag{2}$$

where c is the speed of light in free space, v_g is the group velocity in the medium, and n is the refractive index of the medium [15]. The term f is the filling factor denoting the relative fraction of optical field residing in the analyte medium. Group velocity v_g is inversely proportional to the group index n_g. Hence, theoretically, the optical absorbance by a waveguide on a chip increases in order as follows in silicon: (a) ridge waveguides, ($n_g \sim 3$), (b) slotted ridge waveguides ($n_g \sim 3, f \sim 10$) since the intensity of light in a low-index slot is significantly enhanced compared to ridge waveguides, (c) PCWs ($n_g \sim 100$) [16], and (d) slotted PCWs ($f \sim 10$ and $n_g \sim 100$ for a combined factor of ~1000).

The multiplexed device comprises two 300 μm long PCWs fabricated in the two output arms of a 1×2 multimode interference (MMI) power splitter. In contrast to end-fire coupling used previously, light is coupled into the MMI via an input subwavelength grating (SWG) from a single input optical fiber. Our studies indicate that coupling losses are minimized by the use of SWGs [17]. At the output of the PCWs, the waveguides are combined with a Y-junction power combiner [18]. At the output, the combined transmission spectra from each PCW are coupled via an output SWG to a single output optical fiber. In Fig. 1(a), a stitched image of the whole device is shown. Y-junction combiner, PCW, and MMI regions are magnified in Figs. 1(b)–1(d), respectively.

A 2 μm thick SU-8 polymer is spun on top of the device. Since SU-8 is hydrophobic, the absorption spectrum of VOCs can be obtained independent of any interference from the strong absorbance signatures of water. In contrast to our previous method using PDMS [3], SU-8 was used since it has low optical absorption loss in the wavelength range of interest between 1.62 and 1.7 μm, resulting in high signal-to-noise ratio. All component devices in Fig. 1 are thus designed and fabricated with a SU-8 top cladding.

The simulated coupling efficiencies of the SWG to the optical fiber and to air, calculated by eigenmode expansion simulations with CAMFR [17], are shown in Fig. 2(a). Since a single SWG feeds both W1 PCWs, the SWGs are designed to have the maximum coupling efficiency around 1.65 μm so as to cover the absorption spectra of TCE and xylene at 1.644 and 1.674 μm, respectively. Figure 2(b) shows the SEM image of the fabricated

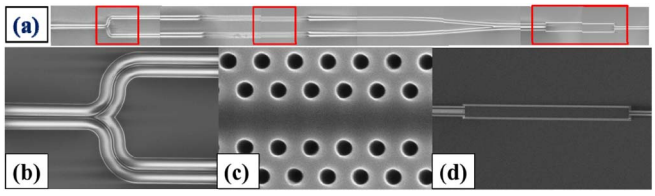

Fig. 1. (a) Stitched scanning electron microscopy (SEM) images of the full device with three regions (red lined) magnified in (b)–(d). (b) Y-junction combiner. (c) W1 line defect PCW. (d) MMI Optical power splitter.

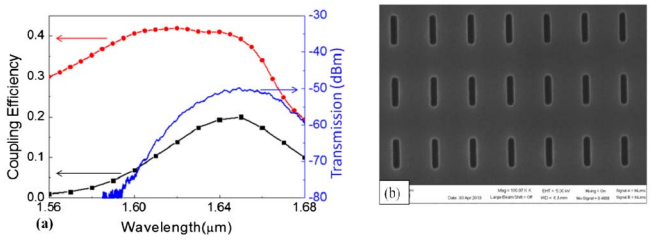

Fig. 2. (a) Simulated coupling efficiency to air (red curve), to the fiber (black curve), and the experimental transmission of the strip waveguide (blue curve) show the coupling peak is located around 1.65 μm. (b) SEM image showing SWG structure.

SWG. The two-dimensional (2D) SWG periods are chosen as 426 and 695 nm along and perpendicular to the waveguide propagation direction. The corresponding trench widths are 79 and 340 nm, respectively. The design results in an effective subwavelength refractive index (n_{sub}) of 2.58 in the propagation direction. The general design of SWG is described in [17]. The resultant transmission spectrum, shown in Fig. 2(a) by the plot in blue, has a maximum transmission near 1.65 μm.

The MMI is designed with a width of 16 μm and a length of 214 μm to achieve optimum 1×2 optical power splitting as shown by the simulation in Fig. 3(b). A schematic W1 PCW with lattice constant a is shown in Fig. 3(a), where W1 denotes that the width of the PCW is $\sqrt{3}a$. Since the absorption peaks of TCE and xylene are located at 1.644 and 1.674 μm, respectively, devices are designed with band edges adjacent to the absorption peaks. Thus, maximum slow light enhancement can be obtained at the absorbance peaks for maximum sensitivity. For xylene, $a = 403$ nm while for TCE $a = 395$ nm. The air hole diameter is $0.53a$ in both PCW arms.

In Fig. 4, the transmission spectrum of the multiplexed PCW device is shown. The design achieves a transmission band with a band edge near 1644 nm (in blue) from one

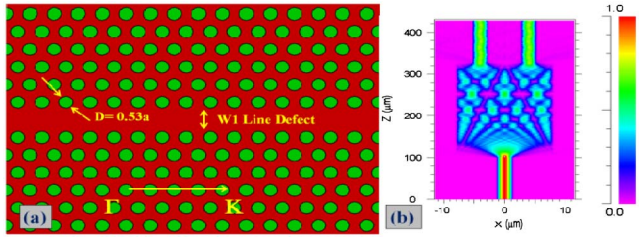

Fig. 3. (a) Schematic of W1 line defect PCW. (b) Beam propagation simulation of the designed 1×2 MMI.

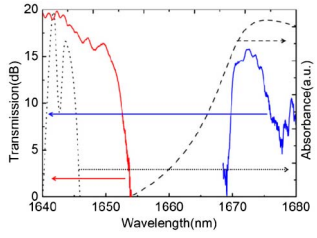

Fig. 4. Transmission of single PC devices with $a = 395$ nm (red curve) and $a = 403$ nm (blue curve). Theoretical absorbance is shown for TCE with peak at 1644 nm (dotted curve) and xylene with peak at 1674 nm (dashed curve).

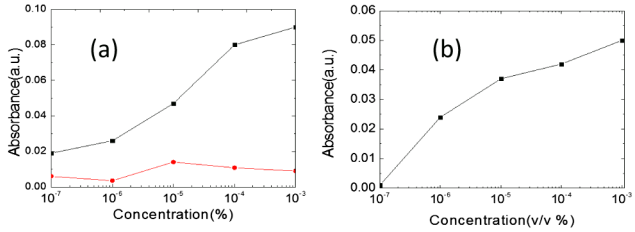

Fig. 5. (a) Absorbance of xylene measured at 1674 nm with PC waveguide (black curve) and strip waveguide (red curve). (b) Absorbance of TCE measured at 1644 nm.

PCW and another band edge near 1674 nm (in red) from the second PCW in the other arm of the MMI. The location of the band edges are indicated by the respective arrows. The variation from the design is attributed to fabrication-induced errors. The theoretical absorbance spectra are indicated in dashed and dotted curves for TCE [19] and xylene [20], respectively. Based on previous results which show that guided wave propagation is obtained in PCWs in SOI platform up to $n_g \sim 35$ with low loss, at the transmission band edge [21], transmitted light being negligible at higher n_g, it is estimated from simulations, that the group indices of the guided mode at 1644 and 1674 nm for the individual waveguides are 23 and 33, respectively.

Figures 5(a) and 5(b) show the experimentally determined absorbance of xylene and TCE from the individual PCWs of Fig. 4 when the device is immersed in water. The 2 μm thick SU-8 ensures negligible overlap of the propagating optical mode with ambient water. Increasing concentrations of xylene and TCE are added separately. The absorbance increases with time when a higher concentration is added. All measurements are done 10 min after sample addition, which is a typical time observed in measurements beyond which no further change in absorbance is observed. The absorbance is calculated by comparing the transmitted light output at each concentration to the transmitted light intensity with no VOC. From the absorbance, the detection limit for device for xylene is 10^{-7}% (v/v) in water (~1 ppb) and the detection limit for device for TCE is 10^{-6}% (v/v) in water (~10 ppb). Measurements in xylene were also done on a ridge waveguide on a chip with no PCW. Negligible absorbance was observed as shown in the red plot in Fig. 5(a).

For multiplexed detection of xylene and TCE, in order to test the selectivity of our device, 10^{-5}% (v/v) xylene in water was added on the multiplexed devices. The transmission is measured from the multiplexed device and the absorbance calculated at 1674 and 1644 nm for xylene and TCE, respectively. In Fig. 6(a), the multiplexed device shows a flat and almost zero

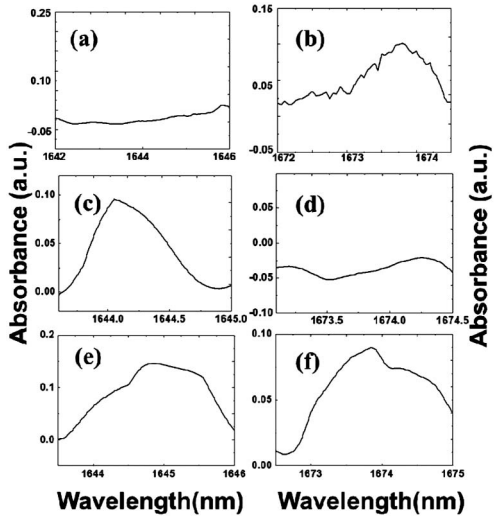

Fig. 6. Absorbance after sequentially adding (a) and (b) 10^{-5}% xylene, (c) and (d) 10^{-5}% TCE, and (e) and (f) 10^{-5}% mixture of xylene and TCE. Absorbance of TCE and xylene are measured at 1644 and 1674 nm, respectively.

absorbance at 1644 nm, but significant absorbance is observed at 1674 nm in Fig. 6(b). Next, a solution of 10^{-5}% (v/v) TCE in water is added on these two devices. In Fig. 6(c), the device shows an absorbance near 1644 nm. In contrast, there is almost flat absorbance for the device designed for xylene in Fig. 6(d). Finally, a mixture of 10^{-5}% xylene (v/v) and 10^{-5}% TCE (v/v) in water was prepared and the solution added. In Figs. 6(e) and 6(f), the absorbance of both xylene and TCE are observed.

The negligible absorbance observed from ridge waveguides of the same total length between input and output SWGs as the multiplexed device in Fig. 1 with PCW shows that the increased absorbance is due to the slow light effect in the PCW. Since SU-8 is more transparent optically than PDMS in the near-IR range probed here, by using SU-8 as the hydrophobic layer, the signal-to-noise ratio was effectively enhanced at the measured wavelengths which therefore lowered the detection sensitivity of our device to 1 ppb for xylene compared to 100 ppb previously [3]. Table 1 compares detection sensitivities experimentally observed in other platforms versus our PCW-based on-chip absorption spectroscopy sensor. More than an order of magnitude enhancement in sensitivity is observed.

The lower sensitivity of TCE is due to fabrication-induced errors that shift the transmission band edge from design values and therefore result in a lower group index at 1644 nm at the absorbance maxima of TCE. While

Table 1. Comparison of Different Methods and Detection Limits of VOCs in Water

Author	Method	Sensitivity
Lai *et al.*, 2011 [3]	PCSW absorption spectroscopy with PDMS	100 ppb (xylene)
Reddy *et al.*, 2012 [7]	μGC	28 ppb (toluene)
Girschikofsky *et al.*, 2012 [9]	Optical planar Bragg grating	20 ppm (xylene), 70 ppm (toluene)
St-Gelais *et al.*, 2013 [10]	Fabry–Perot interferometers	1.6 ppm (xylene)
Hue *et al.*, 2013 [22]	Nanoporous disks absorbance	20 ppb (benzene), 10 ppb (xylene)
Lai *et al.*, 2013 (this Letter)	PCW absorption spectroscopy with SU-8	1 ppb (xylene), 10 ppb (TCE)

10 ppb was experimentally measured, based on the absorbance magnitude in Fig. 5(b), it is estimated that the sensitivity for TCE is better than 10 ppb. We demonstrated the highest sensitivity among existing technologies for the detection of xylene with near-IR absorbance signatures. Since absorbance signatures are larger in the mid-IR, higher sensitivities can be expected if above multiplexed devices are fabricated in the mid-IR. Higher sensitivities are expected to be observed as per Eqs. (1) and (2) in a PC slot waveguide with SU-8 as the SPME layer. Higher multiplexing can be achieved with higher order MMI and Y-junction power splitters and combiners to simultaneously detect more VOCs with selectivity [23].

In summary, we demonstrated multiplexed detection of TCE and xylene in water using PC-based chip-integrated optical absorption spectroscopy. Remote, continuous monitoring is enabled by optical fibers. The authors acknowledge NSF for supporting this work (Grant No. IIP-1127251).

References

1. M. Lackner, Rev. Chem. Eng. **23**, 65 (2007).
2. F. Adler, P. Maslowski, A. Foltynowicz, K. C. Cossel, T. C. Briles, I. Hartl, and J. Ye, Opt. Express **18**, 21861 (2010).
3. W.-C. Lai, S. Chakravarty, X. Wang, C. Lin, and R. T. Chen, Appl. Phys. Lett. **98**, 023304 (2011).
4. W.-C. Lai, S. Chakravarty, X. Wang, C. Lin, and R. T. Chen, Opt. Lett. **36**, 984 (2011).
5. K. M. G. Lima, I. M. Raimundo, and M. F. Pimentel, Sens. Actuators B **125**, 229 (2007).
6. J. Buerck, S. Roth, K. Kraemer, M. Scholz, and N. Klaas, J. Hazard. Mater. **83**, 11 (2001).
7. K. Reddy, Y. Guo, J. Liu, W. Lee, M. K. K. Oo, and X. Fan, Lab Chip **12**, 901 (2012).
8. C.-J. Lu, W. H. Steinecker, W.-C. Tian, M. C. Oborny, J. M. Nichols, M. Agah, J. A. Potkay, H. K. L. Chan, J. Driscoll, R. D. Sacks, K. D. Wise, S. W. Pang, and E. T. Zellers, Lab Chip **5**, 1123 (2005).
9. M. Girschikofsky, M. Rosenberger, S. Belle, M. Brutschy, S. R. Waldvogel, and R. Hellmann, Sens. Actuators B **171**–172, 338 (2012).
10. R. St-Gelais, G. Mackey, J. Saunders, J. Zhou, A. Leblanc-Hotte, A. Poulin, J. A. Barnes, H.-P. Loock, R. S. Brown, and Y.-A. Peter, Sens. Actuators B **182**, 45 (2013).
11. M. Deng, C.-P. Tang, T. Zhu, Y.-J. Rao, L.-C. Xu, and M. Han, Appl. Opt. **49**, 1593 (2010).
12. Q.-Y. Cai and E. T. Zellers, Anal. Chem. **74**, 3533 (2002).
13. D. Matatagui, J. Marti, M. J. Fernandez, J. L. Fontecha, J. Gutierrez, I. Gracia, C. Cane, and M. C. Horrillo, Sens. Anal. Chem. **154**, 199 (2011).
14. J. Liu, Y. Sun, D. J. Howard, G. Frye-Mason, A. K. Thompson, S.-J. Ja, S.-K. Wang, M. Bai, H. Taub, M. Almasri, and X. Fan, Anal. Chem. **82**, 4370 (2010).
15. N. A. Mortensen and S. S. Xiao, Appl. Phys. Lett. **90**, 141108 (2007).
16. M. Notomi, K. Yamada, A. Shinya, J. Takahashi, C. Takahashi, and I. Yokohama, Phys. Rev. Lett. **87**, 253902 (2001).
17. X. Xu, H. Subbaraman, J. Covey, D. Kwong, A. Hosseini, and R. T. Chen, Appl. Phys. Lett. **101**, 031109 (2012).
18. S. H. Tao, Q. Fang, J. F. Song, M. B. Yu, G. Q. Lo, and D. L. Kwong, Opt. Express **16**, 26 (2008).
19. A. C. R. Pipino, J. P. M. Hoefnagels, and N. Watanabe, J. Chem. Phys. **120**, 2879 (2004).
20. D. A. Burns, *Handbook of Near-Infrared Analysis*, 3rd ed. (Taylor & Francis Ltd., 2007).
21. C.-Y. Lin, X. Wang, S. Chakravarty, B. S. Lee, W.-C. Lai, and R. T. Chen, Appl. Phys. Lett. **97**, 183302 (2010).
22. J. Hue, M. Dupoy, T. Bordy, R. Rousier, S. Vignoud, B. Schaerer, T.-H. Tran-Thi, C. Rivron, L. Mugherli, and P. Karpe, "Benzene and xylene detection by absorbance in the range of 10–100 ppb application: quality of indoor air," http://dx.doi.org/10.1016/j.snb.2013.03.047 (2013).
23. A. Hosseini, D. Kwong, C. Lin, B. S. Lee, and R. T. Chen, IEEE J. Sel. Top. Quantum Electron. **16**, 61 (2010).